THE JOURNAL OF BIOLOGICAL CHEMISTRY VOL. 286, NO. 18, pp. 15716–15727, May 6, 2011

Intertissue Flow of Glutathione (GSH) as a Tumor Growth-promoting Mechanism

*INTERLEUKIN 6 INDUCES GSH RELEASE FROM HEPATOCYTES IN METASTATIC B16 MELANOMA-BEARING MICE**

Received for publication, October 20, 2010, and in revised form, February 7, 2011 Published, JBC Papers in Press, March 10, 2011, DOI 10.1074/jbc.M110.196261

Elena Obrador[‡], María Benlloch[§], José A. Pellicer[‡], Miguel Asensi[‡], and José M. Estrela[‡1]

From the [‡]Department of Physiology, University of Valencia, 46010 Valencia, Spain and the [§]Faculty of Experimental Sciences, San Vicente Martir Catholic University, 46001 Valencia, Spain

B16 melanoma F10 (B16-F10) cells with high glutathione (GSH) content show high metastatic activity *in vivo*. An intertissue flow of GSH, where the liver is the main reservoir, can increase GSH content in metastatic cells and promote their growth. We have studied here possible tumor-derived molecular signals that could activate GSH release from hepatocytes. GSH efflux increases in hepatocytes isolated from mice bearing liver or lung metastases, thus suggesting a systemic mechanism. Fractionation of serum-free conditioned medium from cultured B16-F10 cells and monoclonal antibody-induced neutralization techniques facilitated identification of interleukin (IL)-6 as a tumor-derived molecule promoting GSH efflux in hepatocytes. IL-6 activates GSH release through a methionine-sensitive/organic anion transporter polypeptide 1- and multidrug resistance protein 1-independent channel located on the sinusoidal site of hepatocytes. Specific siRNAs were used to knock down key factors in the main signaling pathways activated by IL-6, which revealed a STAT3-dependent mechanism. Our results show that IL-6 (mainly of tumor origin in B16-F10-bearing mice) may facilitate GSH release from hepatocytes and its interorgan transport to metastatic growing foci.

Glutathione (L-γ-glutamyl-L-cysteinyl-glycine; GSH),[2] the most prevalent non-protein thiol in mammalian cells, is involved in many cellular functions (1, 2). GSH in cancer cells is particularly relevant in the regulation of 1) carcinogenic mechanisms; 2) sensitivity against cytotoxic drugs, ionizing radiation, and some cytokines; 3) DNA synthesis; and 4) cell proliferation and death (3, 4).

Early studies on the organ distribution of metastatic cells showed that less than 0.1% of circulating cells survive to cause secondary metastatic growth (5). The liver is a common site for metastasis development, and, as previously shown, a high percentage of circulating cancer cells are mechanically trapped in the liver microvasculature (6). Interaction of metastatic cancer cells with the hepatic sinusoidal endothelium and Kupffer cells activates local release of proinflammatory cytokines, which then may act as molecular signals promoting cancer cell adhesion, invasion, and proliferation (3, 7). Direct *in vitro* lysis of metastatic tumor cells by cytokine-activated murine vascular endothelial cells has also been shown (8).

From the original subcutaneous B16 melanoma tumor, spontaneously originated in C57BL/6J mice, and using sequential *in vitro-in vivo* growing cycles, I. J. Fidler (9) obtained 10 different cell variants (F1–F10) with increasing metastatic potentials. The B16-F10 line showed the highest metastatic activity and became a classical model widely used in metastasis research. Recent results identified the existence of a natural defense mechanism against cancer metastasis whereby the arrest of tumor cells in the liver induces endogenous NO and H_2O_2 release, leading to sinusoidal tumor cell killing and reduced hepatic metastasis formation (3, 10). We have shown that GSH protects circulating B16 cells against hepatic sinusoidal endothelium-induced cytotoxicity (11). By comparing B16 cells cultured to low *versus* high density, which have different GSH contents and different metastatic activities, we found that NO was particularly tumoricidal in the presence of H_2O_2 (a mechanism involving formation of potent oxidants, probably $^{\bullet}OH$ and -OONO, via a trace metal-dependent process) (10). A high percentage of tumor cells with high GSH content survived the combined nitrosative and oxidative attack and probably represent the main task force in the metastatic invasion (12).

Regulation of GSH levels *in vivo* must be looked at in terms of the entire organism, with some organs being net synthesizers of GSH, whereas others are net exporters (3). GSH levels in mammalian tissues normally range from 0.1 to 10 mM, being most concentrated in liver (up to 10 mM). One of the most important functions of GSH is to store Cys because this amino acid is extremely unstable extracellularly and rapidly auto-oxidizes to cystine (13). In rapidly growing tumors, cyst(e)ine, whose concentration in blood is low, may become limiting for GSH synthesis and cell growth (14, 15). Thus, malignant cells might require alternative pathways to ensure free cyst(e)ine availability.

γ-Glutamyl transpeptidase (GGT) cleaves extracellular GSH, releasing γ-glutamyl amino acids and cysteinylglycine, which is further cleaved by membrane-bound dipeptidases into cysteine

* This research was supported by Ministerio de Ciencia e Innovación, Spain, Grants SAF2009-07729 and IPT-010000-2010-21.

[1] To whom correspondence should be addressed: Dept. of Physiology, Faculty of Medicine and Odontology, University of Valencia, 15 Av. Blasco Ibañez, 46010 Valencia, Spain. Tel.: 34-963864649; Fax: 34-963864642; E-mail: jose.m.estrela@uv.es.

[2] The abbreviations used are: GSH, glutathione; B16-F10, B16 melanoma F10 subline; GGT, γ-glutamyl transpeptidase; RFP, red fluorescent protein; B16-F10-RFP, B16-F10 clones expressing the RFP; CM, serum-free conditioned DMEM; KHBM, Krebs-Henseleit bicarbonate medium; MGSA, melanoma growth-stimulatory activity; NTCP, sodium-taurocholate cotransporting polypeptide.

and glycine (16, 17). Free γ-glutamyl-amino acids, cysteine, and glycine entering the cell serve as GSH precursors (18). Hence, GGT expression provides tumor cells with a growth advantage at physiologic concentrations of cyst(e)ine (14). Consequently, we found that tumor GGT activity and an intertissue flow of GSH, where the liver plays a key role, regulate GSH content of B16 melanoma cells and thereby their metastatic growth (15).

In the liver, GSH is released at high rates into both blood and bile. Nearly half of the GSH released by rat hepatocytes is transported across the sinusoidal membrane into the blood plasma for delivery to other tissues (19). Hepatocellular export of GSH through the sinusoidal side mainly involves Oatp1 (the sinusoidal organic anion transporter polypeptide), MRP1 (multidrug resistance protein 1), and probably another mechanism(s) that remains poorly understood and/or molecularly undefined (20). Oatp1 functions as a GSH/organic solute exchanger, and MRP1 functions as an organic anion export pump, but both only account for a fraction of the total GSH released into the blood. Hepatic GSH release increases in metastatic B16 melanoma-bearing mice (as compared with non-tumor-bearing controls), and this increased release appears to be channeled through an Oatp1/MRP1/MRP2-independent system (15). Nevertheless, the molecular nature of this transport (21) and how metastatic cells may influence its activity are still open questions. In the present report, we studied possible tumor-derived molecular signals that could influence GSH release activity in hepatocytes as well as the intracellular regulatory mechanisms involved. Our results identify interleukin (IL)-6 as a systemic signal promoting GSH release from hepatocytes in metastatic B16-F10 tumor-bearing mice.

EXPERIMENTAL PROCEDURES

Culture of B16-F10 Melanoma Cells—Murine B16-F10 melanoma cells (from the ATCC, Manassas, VA) were cultured in serum-free Dulbecco's modified Eagle's medium (DMEM; Invitrogen), pH 7.4, supplemented with 10 mM HEPES, 40 mM $NaHCO_3$, 100 units/ml penicillin, and 100 μg/ml streptomycin (15). Cells were harvested by incubation for 5 min with 0.05% (w/v) trypsin (Sigma) in PBS (10 mM sodium phosphate, 4 mM KCl, 137 mM NaCl), pH 7.4, containing 0.3 mM EDTA, followed by the addition of 10% calf serum to inactivate the trypsin. Cell numbers were determined using a Coulter Counter (Coulter Electronic Inc., Miami, FL). Cell integrity was assessed by trypan blue exclusion and leakage of lactate dehydrogenase activity (15).

Transfection of Red Fluorescent Protein—The pDsRed-2 vector (Clontech) was used to engineer B16-F10 melanoma clones stably expressing red fluorescent protein (RFP). This vector expresses RFP and the neomycin resistance gene on the same bicistronic message. Cultured B16-F10 cells were transfected before reaching confluence. Transfection of the pDsRed-2 vector was carried out using linear 25-kDa polyethyleneimine (PolySciences, Inc., Warrington, PA), as described for adherent cell lines by the manufacturer. Cells were incubated for 4 h with the polyethyleneimine-DNA complex in 5% of their initial culture medium (DMEM containing 10% fetal calf serum) volume. After that 4-h period, the culture medium volume was restored to 100%. Cells were harvested (as above) 4 days after transfection and subcultured into selective medium that contained 200 μg/ml Geneticin (Invitrogen). The level of Geneticin was increased to 2,000 μg/ml stepwise. High performance cell sorting (DAKO, Copenhagen, Denmark) was used to select Geneticin-resistant B16-F10 clones expressing the RFP (B16-F10-RFP) and showing high fluorescence emission. These cells were seeded in 96-well plates, and their growth was followed by immunofluorescence microscopy to select clones showing stable fluorescence emission.

Animals—Syngenic male C57BL/6J mice (9 weeks old) from Charles River Laboratories (Barcelona, Spain) were fed *ad libitum* on a standard diet (Letica, Barcelona, Spain). Mice were kept on a 12-h light/12-h dark cycle with the room temperature maintained at 22 °C. Procedures involving animals were in compliance with international laws and policies (EEC Directive 86/609 and National Institutes of Health guidelines).

Experimental Metastases—Hepatic or lung metastases were produced by intravenous injection (portal vein or tail vein, respectively) into anesthetized mice (Nembutal, 50 mg/kg intraperitoneally) of 10^5 viable B16-F10-RFP cells suspended in 0.2 ml of DMEM. Mice were cervically dislocated 10 days after tumor cell inoculation. Livers and lungs were fixed with 4% formaldehyde in PBS (pH 7.4) for 24 h at 4 °C and then paraffin-embedded. Metastasis density (mean number of foci/100 mm^3 of organ detected in 15 10 × 10-mm^2 sections/organ) and metastasis volume (mean percentage of organ volume occupied by metastases) were determined as described previously (22).

Isolation of B16-F10 Melanoma Cells from Metastatic Foci—Tissues containing tumor cells were obtained by surgical means. Cell dispersion was carried out in minced tissue by the following sequential procedure: 1) trypsinization (25 mg of fresh tissue/ml in Mg^{2+}- and Ca^{2+}-free PBS supplemented with 0.2% trypsin plus 0.5 mM EDTA plus 5 mM glucose, 3 min at 37 °C); 2) three washes in PBS; 3) collagenase digestion (in PBS supplemented with 0.5 mg of collagenase/ml plus 5 mM glucose, 5 min at 37 °C) (steps 1 and 3 were performed in Erlenmeyer flasks where the gas atmosphere was O_2/CO_2, 19:1). Then cells were washed three times in PBS and resuspended in 1 ml of ice-cold PBS, filtered through a 44-μm pore mesh and analyzed using a MoFlo high performance cell sorter (DAKO). Fluorescent B16-F10-RFP cells were separately gated for cell sorting and collected into individual tissue culture chambered slides (Nalge Nunc International Corp., Naperville, IL). Then the sorted tumor cells were harvested and plated in 25-cm^2 polystyrene flasks (Falcon Labware).

Amino Acid Analysis—Proteins were precipitated by treating 0.1 ml of intracellular compartment or blood with 0.4 ml of 3.75% (w/v) ice-cold sulfosalicylic acid in 0.3 M lithium citrate buffer (pH 2.8). After centrifugation, 0.25 ml of the supernatant was injected into an LKB 4151 amino acid analyzer.

Cystine Uptake—B16-F10 cells were plated in 35-mm culture dishes. At the required times, cells were rinsed three times with prewarmed transport medium (10 mM PBS, pH 7.4, with 0.01% $CaCl_2$, 0.01% $MgCl_2$, and 0.1% glucose). Uptake measurement was initiated by the addition of 1.0 ml of transport medium containing 1 mCi of L-[^{3}H]cystine (PerkinElmer Life Sciences) and nonradioactive cystine (0.5 mM). After incubation at 37 °C, uptake was finished by rinsing several times with ice-cold PBS

until less than 0.001% of the initial radioactivity was present in the supernatant. Cells were then dissolved with 0.5 ml of 0.5 N NaOH, and an aliquot was used for determining radioactivity and another for the protein assay. To correct for trapping, transport at 4 °C was studied in parallel (15).

Preparation and Fractionation of Serum-free Conditioned Medium—Serum-free conditioned DMEM (CM) was obtained from confluent cultures of the B16-F10 melanoma cell line. CM was collected from culture flasks under sterile conditions, and a protease inhibitor mixture from BioVision (Mountain View, CA), containing aprotinin, leupeptin, pepstain A, and phenylmethanesulfonyl fluoride at the concentrations indicated by the manufacturer, was added. The medium was centrifuged at 15,000 × *g* to remove floating cells or cellular debris, and then the supernatant was ultracentrifuged (100,000 × *g*) for 30 min to remove subcellular organelles. The resulting supernatant was lyophilized. When 20 liters of CM were processed in this manner, the lyophilized powder was extracted with 1 N acetic acid at room temperature, dialyzed exhaustively against 0.17 N acetic acid at 4 °C, lyophilized, and stored at −80 °C.

Isolation and Incubation of Hepatocytes—Isolation of hepatocytes from non-tumor-bearing and B16-F10-bearing mice followed the method of Berry and Friend (23). Parenchymal liver cells were purified from the crude cell suspension by density gradient centrifugation in a vertical rotor (24). The crude liver cell suspension (50 mg dry weight in 2 ml) was added to a medium (40 ml) containing 40% (v/v) Percoll, 3% (w/v) defatted bovine serum albumin, 10% DMEM, 10 mmol/liter MOPS, 120 mmol/liter NaCl, 6.7 mmol/liter KCl, 1.2 mmol/liter $CaCl_2$ and adjusted to pH 7.4 with 0.1 N NaOH. Centrifugation was carried out at 4 °C in a Beckman-Coulter Optima XL-100K (73,104 × *g* for 15 min). Metabolic viability and integrity of isolated hepatocytes removed from the gradient medium after centrifugation was assayed as previously described (24). For incubations, hepatocytes (10–12 mg dry weight/ml) were suspended at 37 °C in Krebs-Henseleit bicarbonate medium (KHBM, pH 7.4) containing 1.3 mmol/liter $CaCl_2$. The gas atmosphere was 95% O_2, 5% CO_2.

Culture of Hepatocytes—Isolated hepatocytes (3×10^6) were seeded onto 60-mm culture dishes (Invitrogen) in 4 ml of Williams' medium E (Invitrogen) supplemented with 5 mmol/liter L-Gln, 100 units/ml penicillin, 100 mg/ml streptomycin, 200 units/ml insulin, 1 mmol/liter dexamethasone, and 10% fetal calf serum (Invitrogen). The dishes were incubated at 37 °C in a humidified 5% CO_2 atmosphere for 12 h before starting assays.

Perifusion of Hepatocytes—Isolated mouse hepatocytes, suspended in Williams' medium E, were incubated in a perifusion system similar to that previously described for rat hepatocytes (25). Briefly, a buffer gassed with 95% O_2, 5% CO_2 was constantly pumped by an LKB Multiperpex roller pump (type 2115) to a chamber containing a final volume of 10 ml and 3×10^6 cells/ml. The filter (Amicon YM30, Bedford, MA) was placed at the top of the chamber. The cell suspension was perifused at 37 °C and maintained homogenous by using a magnetic stirrer placed at the bottom of the chamber. The perifusion buffer was KHBM (pH 7.4) containing plasma concentrations (aortic blood) of L-amino acids found in non-tumor-bearing C57BL/6J mice (377 ± 42 μmol/liter Ala, 53 ± 12 μmol/liter Asn, 22 ± 6 μmol/liter Asp, 7 ± 1 μmol/liter cyst(e)ine, 79 ± 15 μmol/liter Glu, 467 ± 46 μmol/liter Gln, 233 ± 28 μmol/liter Gly, 41 ± 13 μmol/liter His, 68 ± 9 μmol/liter Ile, 72 ± 14 μmol/liter Leu, 245 ± 33 μmol/liter Lys, 40 ± 9 μmol/liter Met, 52 ± 14 μmol/liter Phe, 124 ± 21 μmol/liter Pro, 83 ± 20 μmol/liter Ser, 121 ± 17 μmol/liter Thr, 72 ± 10 μmol/liter Trp, 87 ± 15 μmol/liter Tyr, 103 ± 12 μmol/liter Val, 114 ± 22 μmol/liter Arg; $n = 15$), glucose (1 g/liter), and sodium pyruvate (10 mg/liter), supplemented with 10 units/ml penicillin and 10 mg/ml streptomycin. Perifusate flow (2 ml/min) was constant throughout the experiment. Effluent flow was monitored continuously for O_2 and pH with Philips electrodes. Cell viability was always greater than 95% along the experimental time. To take samples (0.5 ml) of the cell suspension without interrupting the flow, a syringe was introduced into the chamber through a rubber septum.

Measurement of Cytokine Levels—Blood samples (see below) were centrifuged at 14,000 rpm for 10 min at 4 °C to separate the serum. Concentrations of IL-1α, IL-1β, IL-2, IL-6, IL-10, IL-12, tumor necrosis factor (TNF)-α, and interferon (IFN)-γ in CM samples and of IL-6 in the serum were determined using commercially available mouse cytokine ELISA kits from Innovative Research (Novi, MI). Likewise, concentrations of vascular endothelium growth factor (VEGF)-A, transforming growth factor (TGF)-β, platelet-derived growth factor (PDGF)-B, and melanoma growth-stimulatory activity (MGSA) were measured using mouse ELISA kits from Uscn Life Science Inc. (Wuhan, China), Cell Sciences (Canton, MA), R&D Systems Europe Ltd. (Abingdon, UK), and Antibodies-online GmbH (Aachen, Germany), respectively. The recommended protocol of each manufacturer was followed in all cases. Results were read with a Dynex MRXII ELISA reader (ThermoLabsystems, Chantilly, VA). Quantification of secreted cytokines was accomplished by normalization of the ELISA data with a standard cytokine dose curve.

Cytokine Neutralization Assay—Anti-TNFα, -IFNγ, -IL-2, -IL-18, and -VEGF-A monoclonal antibodies (mAbs) were obtained from Santa Cruz Biotechnology, Inc. (Santa Cruz, CA). Anti-IL-1α, -IL-1β, -IL-6, and -IL-10 mAbs were from BioLegend (San Diego, CA). Anti-MGSA mAbs were from Leinco Technologies, Inc. (St. Louis, MO). Anti-TGF-β and -PDGF-B mAbs were from GenScript (Piscataway, NJ). Serial dilutions of mAbs in PBS, pH 7.4, were added to melanoma cell cultures, and standard protocols from eBioscience (San Diego, CA) for *in vitro* cytokine neutralization were followed.

Determination of GSH and GSSG—GSH and glutathione disulfide in tumor and non-tumor tissues were determined, following procedures described previously (26), by liquid chromatography-mass spectrometry using a Quattro micro™ triple-quadrupole mass spectrometer (Micromass, Manchester, UK) equipped with a Shimadzu LC-10ADVP pump and SCL-10AVP controller system with an SIL-10ADVP autoinjector (Shimadzu Corp., Kyoto, Japan). Tissue/blood sample collection and processing were performed according to a published methodology (27), where rapid *N*-ethylmaleimide derivatization was used to prevent GSH auto-oxidation.

Transfection of Small Interfering RNA—The PSilencer 3.1-H1 linear vector from Ambion Inc. (Austin, TX) was used to obtain long term gene silencing. The siRNA molecules targeting IL-6 mRNA were purchased from Ambion. The RNA duplex against IL-6 had the sequence 5′-GGA CAU GAC AAC UCA UCU CTT-3′ (sense) and 5′-GAG AUG AGU UGU CAU GUC CTG-3′ (antisense). The negative control vector that expresses a hairpin siRNA with limited homology to any known sequences in mice was provided by the vector kit (Ambion). Recombinant PSilencer 3.1-H1 vector was transformed into competent *E. coli* DH5α (Takara Bio Inc., Shiga, Japan), according to the supplier's protocol, and then bacteria were spread on Luria-Bertani solid medium plates containing 50 μg/ml ampicillin and cultured at 37 °C overnight. The bacteria were harvested, centrifuged, and subjected to SDS-alkaline lysis following standard methods (see the Cold Spring Harbor Protocols Web site). Endotoxins were removed from the lysate by simple extraction-phase separation steps. The plasmid DNA was further purified by adsorption onto silica using the GenElute Endotoxin-free Plasmid Maxiprep Kit (Sigma). The purified DNA was diluted to 1 mg/ml and frozen at −20 °C. Transfection with the pSH1-IL-6 plasmids was performed using a standard lipofection method (see the Cold Spring Harbor Protocols Web site). Stably transfected clones were selected in medium containing 0.5 mg/ml Geneticin (Invitrogen). Established clones were grown in medium supplemented with 10% FCS and 0.5 mg/ml Geneticin. Silencing was confirmed by immunoblotting.

RT-PCR and Detection of mRNA—Total RNA was isolated using the TRIzol kit from Invitrogen and following the manufacturer's instructions. cDNA was obtained using a random hexamer primer and a MultiScribe Reverse Transcriptase kit, as described by the manufacturer (TaqMan RT Reagents, Applied Biosystems, Foster City, CA). A PCR master mix and AmpliTaq Gold DNA polymerase (Applied Biosystems) were then added containing the following specific primers (Sigma-Genosys): *IL-6* (forward, CAG AAT TGC CAT CGT ACA ACT CTT TTC TCA; reverse, AAG TGC ATC ATC GTT GTT CAT ACA); *bax* (forward, CCAGCTGCCTTGGACTGT; reverse, ACCCCCTCAAGACCACTCTT); *bak* (forward, TGAAAAATGGCTTCGGGGCAAGGC; reverse, TCATGATTTGAAGAATCTTCGTACC); *bad* (forward, AGGGCTGACCCAGATTCC; reverse, GTGACGCAACGGTTAAACCT); *bid* (forward, GCTTCCAGTGTAGACGGAGC; reverse, GTGCAGATTCATGTGTGGATG); *bik* (forward, ATTTCATGAGGTGCCTGGAG; reverse, GGCTTCCAATCAAGCTTCTG); *bim* (forward, GCCCCTACCTCCCTACAGAC; reverse, CAGGTTCCTCCTGAGACTGC); *bcl-2* (forward, CTCGTCGCTACCGTCGTGACTTCG; reverse, CAGATGCCGGTTCAGGTACTCAGTC); *bcl-w* (forward, GGTGGCAGACTTTGTAGGTT; reverse, GTGGTTCCATCTCCTTGTTG); *bcl-xl* (forward, GTAAACTGGGGTCGCATTGT; reverse, TGGATCCAAGGCTCTAGGTG); *mcl-1* (forward, GAAAGCTGCATCGAACCATT; reverse, ACATTCCTGATGCCACCTTC); and *GAPDH* (forward, TTC ACC ACC ATG GAG AAG GC; reverse, GGC ATG GAC TGT GGT CAT GA). Real-time quantitation of the mRNA relative to GAPDH was performed with a SYBR Green I assay, and an iCycler detection system (Bio-Rad). Target cDNA was amplified as follows: 10 min at 95 °C and then 40 cycles of amplification (denaturation at 95 °C for 30 s and annealing and extension at 60 °C for 1 min per cycle). The increase in fluorescence was measured in real time during the extension step. The threshold cycle (C_T) was determined, and then the relative gene expression was expressed as follows: -fold change $= 2^{-\Delta(\Delta\ C_T)}$, where $\Delta C_T = C_T$ target $- C_T$ GAPDH, and $\Delta(\Delta C_T) = \Delta C_T$ treated $- \Delta C_T$ control.

Functional Activity of JAK-STAT and MAPK Pathways—For Western immunoblotting studies, cultured hepatocytes, harvested as indicated above, were washed twice in ice-cold KHBM (pH 7.4). Cell extracts were made by freeze-thaw cycles (cells) or homogenization (tissues) in a buffer containing 150 mM NaCl, 1 mM EDTA, 10 mM Tris-HCl, 1 mM phenylmethylsulfonyl fluoride, 1 μg/ml leupeptin, 1 μg/ml aprotinin, and 1 μg/ml pepstatin, pH 7.4. The extracts were centrifuged at 10,000 × *g* for 30 min. Cell/tissue lysate supernatants were separated for protein determination. The protein content was determined by the Bradford assay (28). All steps were performed at 4 °C. Antibodies (mouse monoclonal primary antibodies) against Jak1, phosphotyrosine Jak1 (P-Jak1), STAT1, phosphotyrosine STAT1 (P-STAT1), STAT3, phosphoserine STAT3 (P-STAT3), ERK1/2, phosphothreonine ERK1/2, and β-actin were from Santa Cruz Biotechnology, Inc. Antibodies against p38, phosphothreonine/phosphotyrosine p38 (P-p38), c-Jun, phosphoserine c-Jun (P-c-Jun), c-Fos, and phosphoserine c-Fos (P-c-Fos) were from Cell Signaling Technology (Danvers, MA). Fifty μg of protein were boiled in Laemmli buffer and resolved by 12.0% SDS-PAGE. Proteins were transferred to a nitrocellulose membrane (Hybond C-extra, Amersham Biosciences) and subjected to Western blotting. The blotted membrane was blocked for 1 h at room temperature in Tris-buffered saline (TBS) containing 5% (w/v) membrane blocking reagent (nonfat dried milk). All antibody incubations were carried out at room temperature in TBS containing 1% membrane-blocking reagent. The incubation steps were followed by three washing steps of 5 min with TBS containing 0.1% Tween 20. Blots were developed using horseradish peroxidase-conjugated secondary antibody and enhanced chemiluminescence (ECL system, GE Healthcare). Quantification of the protein bands was carried out using laser densitometry. Equality of protein loading on membranes and complete transfer were checked by staining gels and membranes with Coomassie Blue. To make possible the pooling of data from multiple immunoblots, the relative density of each band was normalized against the internal standard (β-actin) analyzed on each blot. All Western immunoblots were performed at least three times by using nuclear or cytoplasmic extracts.

Antisense oligonucleotides used were as follows: 5′-GGCCTCTCCTGCGACATCTT-3′ for p38; 5′-GCCGCCGCCGCCGCCAT-3′ for ERKs; 5′-CCA CTG AGA CAT CCT GCC ACC-3′ for STAT1; and 5′-GCT CCA GCA TCT GCT GCT TC-3′ for STAT3. As controls, the corresponding sense oligonucleotides and scrambled oligonucleotides were used (29). Oligonucleotides were synthesized using standard phosphorothioate chemistry. To increase stability, oligonucleotides were synthesized with a 2-omethoxyethyl modification of the five

TABLE 1

GSH synthesis and efflux in isolated hepatocytes from non-tumor-bearing and B16-F10 melanoma-bearing mice

The initial GSH concentration was of 4.8 ± 0.3 μmol/g in isolated hepatocytes from non- tumor-bearing mice and of 2.7 ± 0.4 μmol/g in hepatocytes from mice bearing liver or lung metastases ($n = 8–9$ in all cases). Hepatocytes from B16-F10-bearing mice were isolated 10 days after tumor inoculation. Hepatocytes were incubated in 10-ml Erlenmeyer flasks (final volume 2 ml) for 60 min (see "Experimental Procedures") in the presence or in the absence of amino acids (5 mM Gln, 2 mM Gly, 1 mM Ser, 1 mM *N*-acetylcysteine) (22). Only L-amino acids were used. Glucose (5 mM) and bovine serum albumin (2%) were present in all incubations. Rates of GSH synthesis were calculated from total GSH content in incubations at 0, 20, 40, and 60 min. Rates of glutathione efflux were calculated from contents of GSH and GSSG in extracellular medium at 0, 20, 40, and 60 min. All values are means ± S.D. for 8–9 observations. The significance test refers, for both groups, to the comparison of rates in the absence or in the presence of amino acids (**, $p < 0.01$), and also to the difference between results for the B16-F10 group and the non-tumor-bearing group (†, $p < 0.05$; ††, $p < 0.01$).

	GSH synthesis			GSH efflux		
		B16-F10 metastases			B16-F10 metastases	
Additions	Non-tumor	Liver	Lung	Non-tumor	Liver	Lung
	nmol/g × min			*nmol/g × min*		
None	2 ± 0.5	5 ± 2†	4 ± 1	2 ± 0.7	7 ± 3††	7 ± 1††
L-Amino acids	25 ± 6**	22 ± 7**	23 ± 5**	10 ± 3**	20 ± 4**††	18 ± 4**††

terminal nucleotides (30). Transfections of small interfering RNA were carried out as described above.

Nuclear extracts were prepared with a nuclear extraction kit (Millipore, Billerica, MA). The DNA binding activity of STAT-3 in nuclear extract was determined by the STAT3 EZ-TFA transcription factor assay kit (Millipore) according to the manufacturer's protocol.

Taurocholate Uptake into Hepatocytes—Hepatocyte monolayers were washed three times with KHBM (pH 7.4, 37 °C). Uptake studies were initiated by adding 4 ml of KHBM supplemented with 2 mCi of [^{3}H]taurocholic acid (PerkinElmer Life Sciences) and 20 mmol/liter nonradiolabeled taurocholic acid (Calbiochem, Darmstadt, Germany). The incubation period was 2 min because preliminary experiments showed that uptakes were linear (r.0.99) for at least 3 min. Uptake was finished by aspirating the transport buffer and rinsing the culture dishes twice with 4 ml of ice-cold KHBM. This removes more than 99% of extracellular label without affecting intracellular radioactivity. Then 2 ml of Triton X-100 (0.5%, w/v) were added to the dishes, and the cells were solubilized at room temperature. One-milliliter aliquots of the lysates were mixed with 9 ml of toluene (Merck, Darmstadt, Germany), and the cell-associated radioactivity was measured in a TriCarb 2700TR liquid scintillation analyzer (Canberra Packard, Tecnasa, Madrid, Spain).

Laser Microdissection—Excised liver samples were embedded in freezing medium OCT (Tissue-Tek, Electron Microscopy Sciences, Hatfield, PA) and immediately flash-frozen using isopentane and following the instructions of Leica Microsystems (Wetzlar, Germany) to preserve RNA. Five-μm tissue slices were obtained using a Leica 2800E Frigocut Cryostat Microtome. Tumor cells were separated using a Leica LMD6000 laser microdissection system equipped with an automated fluorescence module.

Expression of Results and Statistical Analyses—Data are presented as the means ± S.D. for the indicated number of different experiments. Statistical analyses were performed using Student's *t* test, and *p* values of <0.05 were considered significant.

RESULTS

GSH Synthesis and Release in Hepatocytes from Metastatic Tumor-bearing Mice—The liver is the main source of circulating plasma GSH (over 90% of the total GSH inflow) (18, 31). As compared with non-tumor-bearing mice, GSH levels decrease in the liver and kidney of Ehrlich ascites tumor-bearing mice (32) and in the brain, lung, liver, and kidney of B16-F10-bearing mice (15). We also found that GGT overexpression in B16-F10 cells, by degrading extracellular GSH, facilitates their metastatic growth (15). Therefore, hypothetically, it is plausible that tumor cells may release molecular signals that activate an interorgan flow of GSH (33). Thus, we further investigated if metastatic cells cause changes in the rate of GSH synthesis and/or efflux in hepatocytes. Rates were measured in the absence and in the presence of amino acid precursors for GSH synthesis. This allows comparison between basal rates (those obtained when synthesis *in vitro* just depends on the intracellular available amino acids) and rates obtained in the presence of non-limiting amounts of extracellular precursors (maximal rates). As shown in Table 1, GSH synthesis is similar in isolated hepatocytes from non-tumor-bearing mice and from mice bearing B16-F10 metastases. However, as compared with non-tumor-bearing controls, rates of GSH efflux increase (~2-fold) in hepatocytes isolated from mice bearing B16-F10 metastases (Table 1). Interestingly, this increase occurs in mice bearing liver or lung metastases (Table 1), thus suggesting a systemic mechanism and not merely a paracrine effect.

As shown in Table 2 the increase in hepatic GSH release causes a parallel decrease in hepatic GSH content to ~50% of control values (10 days after tumor inoculation), a finding that was similar in mice bearing B16-F10 lung or liver metastases. However GSH levels in circulating blood also decreased to ~70% of control values, a fact that may reflect extracellular GSH utilization by the tumor cells (15, 34) (see also the Introduction).

Plasmatic (aortic blood) levels of cyst(e)ine in non-tumor-bearing mice and in mice bearing B16-F10 (hepatic metastases; 10 days after inoculation) were 10.5 ± 1.3 and 7.6 ± 1.5 μM ($p < 0.05$), respectively. Cysteine is transported mainly by system ASC (35); thus, changes in amino acid transport affecting this system should be reflected by changes in the plasma concentration of other amino acids transported by the same system. This is not the case because plasma levels of alanine and proline did not change significantly between controls and B16-F10-bearing mice (not shown). Therefore, although not affecting cysteine transport directly, tumors expressing high GGT levels can efficiently degrade plasma GSH, providing abundant cysteine for

TABLE 2

Blood and liver GSH content in mice bearing metastatic B16-F10 melanoma growing at different body sites

Blood was collected from the tail vein into 1-ml syringes containing sodium heparin (0.05 ml of a 5% solution in 6.9% NaCl). Animals were killed 5 or 10 days after inoculation of tumor cells. Metastasis-free liver pieces (selected by visual analysis using a binocular microscope) were quickly dissected and removed, washed at 4 °C in KHBM (pH 7.4) without Ca^{2+} or Mg^{2+} and containing 0.5 mM EGTA, dried on tissue paper, and frozen in liquid nitrogen. Before adding liquid nitrogen, small liver tissue samples were separated for routine analysis by a pathologist. Only real metastatic focus-free liver samples were used for GSH analysis. MV, metastasis volume (mean percentage of organ volume occupied by metastasis). Blood/tissue samples were treated as described under "Experimental Procedures." Data are means ± S.D. for 10–12 different mice. *, $p < 0.05$; **, $p < 0.01$ comparing values obtained in mice bearing B16-F10 metastases *versus* control non-tumor-bearing mice, or 10 *versus* 5 days in liver and lung metastasis volume.

		B16-F10 metastases			
		Liver		Lung	
	Non-tumor (0 days)	5 days[a]	10 days	5 days	10 days
Blood GSH (μmol/g hemoglobin)	7.4 ± 0.6	7.2 ± 0.5	4.8 ± 0.2**	7.3 ± 0.5	5.3 ± 0.3**
Liver GSH (μmol/g of tissue)	7.1 ± 0.5	5.9 ± 0.6*	3.3 ± 0.4**	6.6 ± 0.4	3.5 ± 0.5**
MV (%)		4.2 ± 1.7	17.5 ± 3.9**	3.6 ± 1.4	12.3 ± 2.6**

[a] Days after tumor inoculation.

uptake (15). Besides, plasma concentration of cystine is usually higher than that of cysteine, and cystine is readily converted to cysteine within cells (35). Thus, we also measured uptake of cystine, which enters the cell through the Na^+-independent x_c^- system in exchange for glutamate (35). In B16-F10-RFP cells isolated from hepatic metastases, we found that the intracellular concentration of amino acids was similar 5 or 10 days after cancer cell inoculation. In particular, concentrations of free glutamate and glycine were (*e.g.* in B16-F10 cells 10 days after inoculation) 2.4 ± 0.5 and 1.2 ± 0.4 μM, respectively (which ensures maximal rates of GSH synthesis) (16), whereas glutamine (a major fuel for cancer cells (36)) and cyst(e)ine (cysteine + cystine) (rapidly used for protein and GSH synthesis (22)) were undetectable. However, rates of cystine uptake were significantly different when metastatic B16-F10-RFP cells, 5 and 10 days after inoculation, were compared (0.25 ± 0.08 and 0.36 ± 0.05 nmol of cystine/mg of protein × min, respectively; $p < 0.05$, $n = 4$). Hence, intracellular cysteine availability in metastatic cells appears modulated by its GGT-dependent generation from extracellular GSH and the uptake rate of cystine.

Identification of Tumor-derived Molecular Signals Promoting GSH Efflux in Hepatocytes—Are there molecules released by tumor cells that can reach the liver and activate GSH efflux from hepatocytes? In order to answer this question, we first fractionated serum-free CM from cultured B16-F10 cells (see "Experimental Procedures"). As shown in Table 3, CM>12–25 increased GSH efflux in hepatocytes isolated from non-tumor-bearing mice, whereas CM>45–67 did not. Thus, suggesting that potential B16-F10-derived signals promoting GSH efflux in hepatocytes should correspond roughly to factors with molecular masses of >12.4–25 kDa and <45–67 kDa (see the legend to Table 3). However, CM>12 did not increase GSH efflux in hepatocytes isolated from B16-F10-bearing mice (Table 3), which is not surprising because rates of GSH efflux in these cells were already increased as compared with controls (hepatocytes from non-tumor-bearing mice incubated in the absence of CM). This fact suggests that the potential signaling mechanism was acting *in vivo* in B16-F10-bearing mice previously to isolate their hepatocytes.

Malignant melanoma cells express different growth factors and cytokines and their receptors in respective stages of tumor progression, which by autocrine and paracrine effects enable

TABLE 3

B16-F10 conditioned medium promotes GSH efflux in cultured hepatocytes

B16-F10-RFP cells were isolated from liver metastatic foci and then cultured, as described under "Experimental Procedures." Lyophilized CM (see "Experimental Procedures") was dissolved in DMEM (1 mg/ml) and filtered using microcon centrifugal filter units containing YM-50 (percentages of protein recovery for α-chymotrypsinogen (25 kDa), cytochrome *c* (12.4 kDa), and protamine sulfate (5–10 kDa) were approximately 85, 7, and 2%, respectively) or YM-100 membranes (percentages of protein recovery for bovine serum albumin (67 kDa), ovalbumin (45 kDa), and α-chymotrypsinogen were approximately 90, 11, and 2%, respectively) (Millipore). This procedure generated two CM fractions corresponding to two major molecular weight regions: CM>12–25 and CM>45–67. CM, CM>12–25, and CM>45–67 were added, at different amounts, to cultured hepatocytes. The initial GSH concentration was 4.5 ± 0.3 μmol/g in cultured hepatocytes from non-tumor-bearing mice and 3.4 ± 0.4 μmol/g in cultured hepatocytes from B16-F10-bearing mice ($n = 6$ in both cases). Results are means ± S.D. of 5–6 independent experiments where each sample was run in duplicate. Rates of GSH efflux were calculated from the contents of GSH and GSSG in the extracellular medium at 0, 30, 60, and 120 min of incubation, starting as indicated under "Experimental Procedures." Rates of GSH efflux in hepatocytes isolated from mice bearing B16-F10 lung metastases were not significantly different as compared with the rates displayed in this table under liver metastases (not shown). The significance test refers, for both groups, to the comparison in the absence or in the presence of additions (*, $p < 0.05$; **, $p < 0.01$) and also to the difference between results for the B16-F10 group and the non-tumor-bearing group (†, $p < 0.05$; ††, $p < 0.01$).

Additions	Lyophilized powder added (μg/ml of culture medium)	GSH efflux	
		Non-tumor	B16-F10 (liver metastases)
	μg/ml	*nmol/g × min*	
None	0	9 ± 2	20 ± 4††
CM	10	15 ± 3**	20 ± 3
	25	24 ± 2**	23 ± 2
	50	23 ± 5**	26 ± 3
CM>12.4	10	17 ± 2**	24 ± 3†
	25	26 ± 3**	23 ± 4
	50	25 ± 4**	25 ± 2
CM>45–67	10	8 ± 2	20 ± 3††
	25	10 ± 2	22 ± 3††
	50	7 ± 1	20 ± 2††

them to grow autonomously and confer competence to metastasis (37, 38). Known factors secreted (in significant amounts) by malignant melanoma cells, which are approximately >12 and <67 kDa, include TNFα, IFNγ, different interleukins (IL-1α, IL-1β, Il-2, IL-6, IL-10, and IL-18), VEGF-A, TGF-β, PDGF-B, and MGSA (37, 39, 40). Thus, we measured levels of each of these factors in the culture medium of growing B16-F10 cells (Table 4). As shown in Table 4, mAb-induced cytokine/activity neutralization decreased their levels to less than 5% of controls in all cases. B16-F10 CM increased GSH efflux in cultured hepatocytes isolated from non-tumor-bearing mice (Table 4). However, only IL-6 neutralization significantly decreased GSH efflux in hepatocytes cultured in the presence of

TABLE 4

Effect of cytokine/activity neutralization on B16-F10 conditioned medium-induced GSH efflux in cultured hepatocytes isolated from non-tumor-bearing mice

B16-F10 CM (25 μg/ml hepatocyte culture medium) was added 24 h after hepatocyte seeding. Free cytokine/activity levels in hepatocyte culture medium were measured 6 h after the B16-F10 CM addition. Specific mAbs against each cytokine/activity (see "Experimental Procedures") were added, independently, 24 h after seeding. Controls received an equivalent volume of PBS. Rates of GSH efflux were calculated as indicated in Table 3, starting 48 h after seeding. Results are means ± S.D. of 4–5 independent experiments where each sample was run in duplicate. The significance test refers to the comparison between GSH efflux measured in the presence of B16-F10 CM or B16-F10 CM plus each specific mAb *versus* control GSH efflux (+PBS) (**, $p < 0.01$).

	Cytokine/activity (pg/ml of B16-F10 culture medium)		GSH efflux (nmol/g of hepatocytes × min)		
	+PBS	+mAbs	+PBS	+B16-F10 CM	+B16-F10 CM + mAbs
	pg/ml		*nmol/g × min*		
			8 ± 1	20 ± 2**	
TNFα	889 ± 216	<20			21 ± 4
IFNγ	103 ± 45	<7			23 ± 3
IL-1α	126 ± 38	<10			18 ± 4
IL-1β	47 ± 12	<3			21 ± 2
IL-2	1060 ± 396	<20			20 ± 3
IL-6	3359 ± 917	<30			8 ± 3**
IL-10	362 ± 88	<10			22 ± 5
IL-18	967 ± 204	<15			20 ± 3
MGSA	2703 ± 975	<20			19 ± 3
VEGF-A	40 ± 9	<2			21 ± 3
TGF-β	612 ± 93	<17			19 ± 4
PDGF-B	16 ± 5	<1			22 ± 3

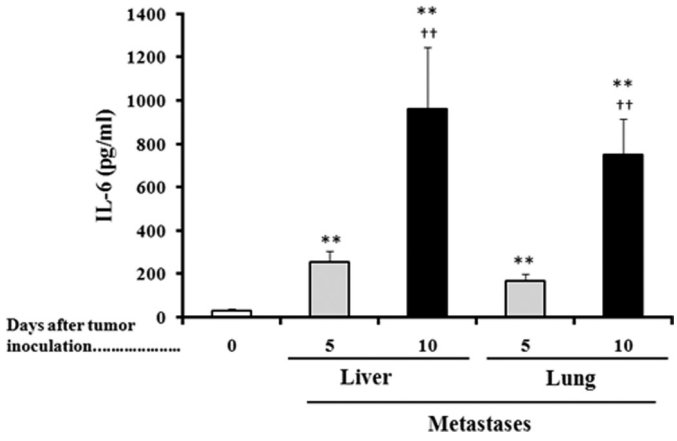

FIGURE 1. **IL-6 levels in serum of non-tumor-bearing and metastic B16-F10-bearing mice.** Blood was collected from the tail vein every 6 h during the 24-h period of each indicated day. Data are mean values of the peak serum cytokine concentrations ± S.D. (*error bars*) (pg/ml) measured in 7–8 different animals. *, $p < 0.05$; **, $p < 0.01$ comparing B16-F10-bearing mice *versus* non-tumor-bearing mice; †, $p < 0.05$; ††, $p < 0.01$ comparing 10 *versus* 5 days after tumor inoculation.

B16-F10 CM (Table 4), thus suggesting that IL-6 (from tumor and probably from non-tumor origin) could be a systemic signal activating GSH release from the liver in tumor-bearing hosts. We measured IL-6 levels in blood serum obtained from non-tumor-bearing mice and from mice bearing liver or lung B16-F10 metastases and found that IL-6 levels increase progressively as metastases grow (Fig. 1; see also Table 2). This progressive increase in serum IL-6 levels (Fig. 1) associates with a decrease in the liver GSH content (Table 2).

Whether the increase in serum IL-6 levels reflects an increased release of this cytokine from the tumor or from non-tumor cells was a question that we addressed in the next step.

TABLE 5

Effect of siRNA-induced tumor IL-6 silencing on hepatic GSH release in B16-F10 tumor-bearing mice

Gene transfections were performed as explained under "Experimental Procedures." Measurements were performed 7 days after tumor cell inoculation. Liver GSH was obtained as in Table 2, serum Il-6 was obtained as described in the legend to Fig. 1, and hepatic GSH efflux (in hepatocytes isolated from the tumor-bearing (lung metastases) mice and incubated in the presence of amino acid precursors) was obtained as in Table 1. IL-6 expression is expressed as -fold change (RT-PCR; see "Experimental Procedures" for calculations). The data show mean values ± S.D. for 5–6 different experiments. *, $p < 0.05$; **, $p < 0.01$ comparing B16-F10/IL-6-siRNA-bearing mice versus control B16-F10-bearing mice.

	Lung metastases	
	B16-F10	B16-F10/IL-6-siRNA
Liver GSH (μmol/g of tissue)	4.5 ± 0.4	6.4 ± 0.5**
Serum IL-6 (pg/ml)	375 ± 83	146 ± 41**
Hepatic GSH efflux (nmol/g of hepatocytes × min)	18 ± 3	12 ± 2*
IL-6 expression (-fold change)	1.0 ± 0.2	0.10 ± 0.05**

For this purpose, we inoculated intravenously (tail vein) control B16-F10 cells and B16-F10 cells transfected with siRNA specific for IL-6 (B16-F10/IL-6-siRNA) to down-regulate IL-6 expression. As shown in Table 5, in metastatic tumor IL-6, silencing causes a significant decrease in circulating IL-6 and in hepatic GSH efflux and consequently an increase in liver GSH content, thus suggesting that tumor-derived IL-6 release is the main factor inducing GSH release form the liver.

Whether this tumor-derived increase in serum IL-6 levels depends upon metastatic activity and/or potential is also an interesting question that we have attempted to investigate. For this purpose, we injected B16-F10 (very high metstatic potential) and B16-F1 (very low metastatic potential), subcutaneously, into syngenic male C57BL/6J mice. Tumors were allowed to grow up to ~200 mm^3 (poorly vascularized) or 800 mm^3 (highly vascularized). No significant metastatic spread was detected in each case. Liver GSH content (as in Table 2) and peak serum IL-6 concentrations (as in Fig. 1) were measured. As compared with controls (non-tumor-bearing mice), where we measured 7.0 ± 0.4 μmol of GSH/g of tissue and 35 ± 12 pg of IL-6/ml of serum, we only found significant differences in mice bearing 800-mm^3 B16-F10 tumors (3.5 ± 0.6 μmol of GSH/g of tissue and 712 ± 126 pg of IL-6/ml of serum; $p < 0.01$) ($n = 4–5$ in all conditions). These data suggest that 1) not metastatic tumors but the metastatic phenotype appears important in order to develop the capacity to export IL-6 from the tumor to the blood; 2) small/poorly vascularized tumors, even having high metastatic potential, do not show that capacity under *in vivo* conditions. Whether other systemic signal(s), specific tissue microenvironment, and/or endothelial cell interactions with the cancer cells may also play roles in regulating that capacity are possibilities that should be explored.

IL-6 Induces GSH Release through a Methionine-sensitive Channel—GSH efflux in hepatocytes from B16-F10-bearing mice (~2-fold higher than controls; Table 1) is not inhibited by rifamycin SV or rifampicin (inhibitors of Oatp1 and/or Oatp2), although both inhibited taurocholate uptake (15). Moreover, abrogation ($MRP1^{-/-}$ or $MRP2^{-/-}$ knock-out clones) of MRP1 or MRP2 GSH efflux did not affect the rate of GSH release in hepatocytes from B16-F10-bearing mice (15). However, this GSH efflux was significantly inhibited by methionine (15). In the present report, we investigated if methionine affects

TABLE 6

Effect of IL-6, perifused at *in vivo* serum concentrations, on GSH efflux in hepatocytes isolated from non-tumor-bearing and metastic (lung metastases) B16-F10-bearing mice

Hepatocytes were isolated and perifused for 12 h as described under "Experimental Procedures." IL-6 (960 pg/ml; see data in Fig. 1) was present in the perifusion buffer during the last 6 h. Cell viability within the perifusion chamber remained >95% either in the absence or in the presence of IL-6. After the 12-h period of perifusion, hepatocytes were taken from the perifusion chamber and cultured as described under "Experimental Procedures." Rates of GSH efflux were measured in cultured hepatocytes 48 h after seeding and calculated as indicated in Table 3. Results are means ± S.D. of 4–5 independent experiments where each sample was run in triplicate. The significance test refers to the comparison (*a*) in the absence or in the presence of additions (**, $p < 0.01$), (*b*) in the absence or in the presence of Il-6 (††, $p < 0.01$), and (*c*) of B16-F10- bearing metastases *versus* non-tumor-bearing controls ($^{\#\#}$, $p < 0.01$).

	GSH efflux			
	Non-tumor		B16-F10 (lung metastases)	
Additions	Without IL-6	With IL-6	Without IL-6	With IL-6
	nmol/g × min			
None	9 ± 2	18 ± 3††	20 ± 4$^{\#\#}$	21 ± 3
Methionine (1 mM)	3 ± 1**	9 ± 2**††	9 ± 3**$^{\#\#}$	12 ± 3**
Methionine (1 mM) + acivicin (0.1 mM)	4 ± 0.5**	10 ± 2**††	12 ± 2**$^{\#\#}$	13 ± 2**

IL-6-induced GSH efflux. For this purpose, a perifusion chamber, containing a suspension of hepatocytes, was used as an experimental set-up that mimics *in vivo* conditions by providing a constant supply of glucose, amino acids, and IL-6 at plasma concentrations (see "Experimental Procedures"). As shown in Table 6, methionine inhibits GSH release in perifused hepatocytes (either isolated from control non-tumor-bearing mice or from mice bearing B16-F10 metastases). Methionine-induced inhibition was also assayed in the presence of acivicin (an irreversible GGT inhibitor) (41) to prevent possible GGT-catalyzed degradation of extracellular GSH. However, due to the low GGT activity present in the liver (42), no significant differences were found comparing methionine plus acivicin *versus* methionine (Table 6). Therefore, our results indicate that the cytokine-induced GSH release in hepatocytes from metastatic tumor-bearing mice is channeled through a putative methionine-sensitive system.

IL-6 and the JAK-STAT and MAPK Signaling Pathways—In the liver, IL-6, after its binding to the IL-6 receptors on the cell surface, activates different signaling pathways. In one pathway, IL-6 binding leads to the rapid association of the transmembrane IL-6 receptors and intracellular glycoprotein 130 (gp130), followed by the activation of receptor-associated Janus-activated kinases (JAKs). The activated JAKs induce self-phosphorylation on tyrosine residues and the tyrosine phosphorylation of the IL-6 receptor, gp130, and a family of transcription factors termed signal transducers and activators of transcription (STATs). The activated STAT proteins, mainly STAT1 and STAT3, then dimerize, translocate to the nucleus, and play an important role in inducing or modulating the transcription of multiple genes (43, 44). Activation of the IL-6 receptor also stimulates a second pathway, which involves various members of the mitogen-activated protein kinase (MAPK) family, including extracellular signal-regulated kinase 1 (ERK1), ERK2, and p38 stress-activated protein kinase (p38) (43, 44). Hence, we assessed the influence of the metastatic

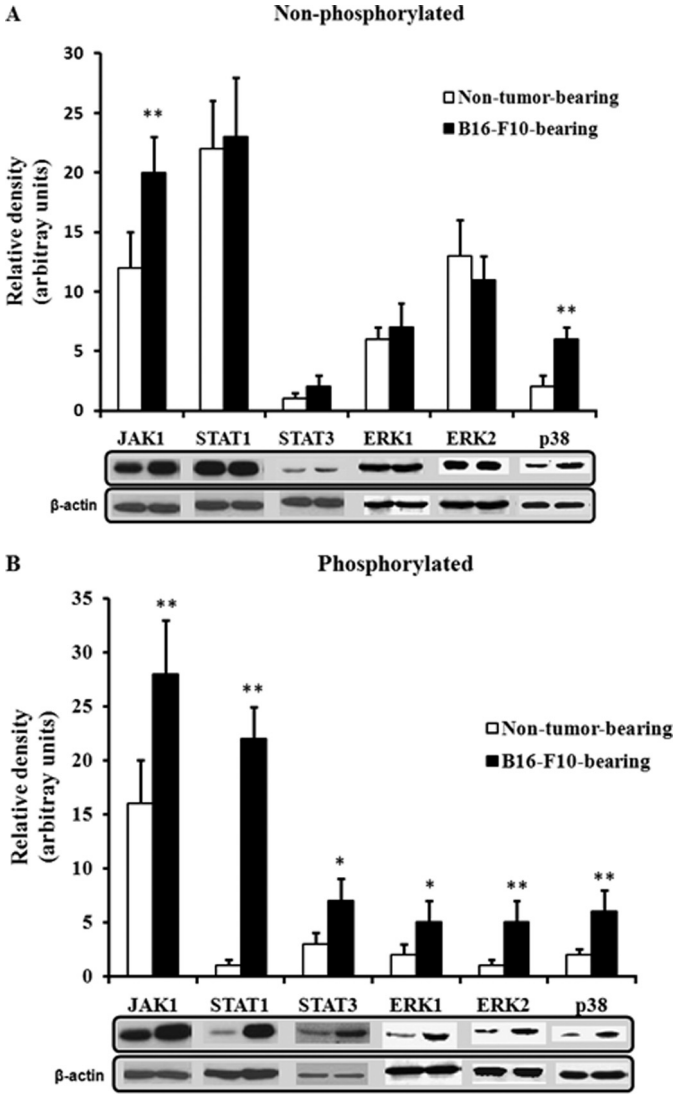

FIGURE 2. **Activation of JAK-STAT and MAPK signaling pathways in hepatocytes of metastatic B16-F10 melanoma-bearing mice.** Hepatocytes from B16-F10 (lung metastases)-bearing mice were isolated 10 days after tumor inoculation. Western blot analyses were performed, using specific antibodies, as described under "Experimental Procedures." Each *lane* in the blots corresponds to an individual representative animal in the indicated group. Results of quantitative analysis of immunoblots are means ± S.D. (*error bars*) for 4 mice/group expressed as relative changes in arbitrary densitometry units normalized against an internal standard (β-actin). *, $p < 0.05$; **, $p < 0.01$ comparing B16-F10 *versus* non-tumor.

B16-F10 tumor on the activation status or levels of JAK1, STAT1, STAT3, ERK1, ERK2, and p38, which are some pivotal factors in the main signaling pathways activated by IL-6 in the liver (43, 44). As shown in Fig. 2, phosphorylated levels of JAK-STAT and MAPK pathway-related factors were higher in hepatocytes of mice bearing B16-F10 metastases than in hepatocytes isolated from non-tumor-bearing mice. Nevertheless, in order to identify which pathway links IL-6 and GSH efflux, we used transfection of specific siRNA to knock down in hepatocytes several of the key factors in the main signaling pathways. Silencing (less than 10% of controls in all cases) was confirmed by immunoblotting (not shown). As shown in Fig. 3, in hepatocytes isolated from mice bearing B16-F10 metastases, only STAT3-siRNA decreased GSH

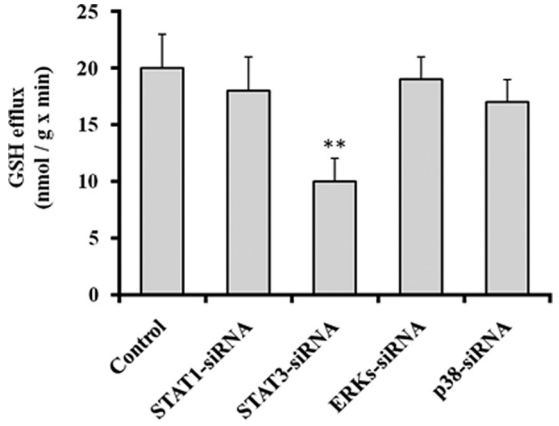

FIGURE 3. **Effect of siRNA-induced STAT1, STAT3, ERKs, or p38 silencing on GSH efflux in hepatocytes isolated (10 days after tumor inoculation) from B16-F10 (lung metastases)-bearing mice.** Gene transfections were performed as explained under "Experimental Procedures." Rates of GSH efflux were measured in cultured hepatocytes 48 h after seeding, and calculated as indicated in Table 3. Results are means ± S.D. (*error bars*) of 4–5 independent experiments where each sample was run in triplicate. **, $p <$ 0.01 comparing each condition *versus* controls.

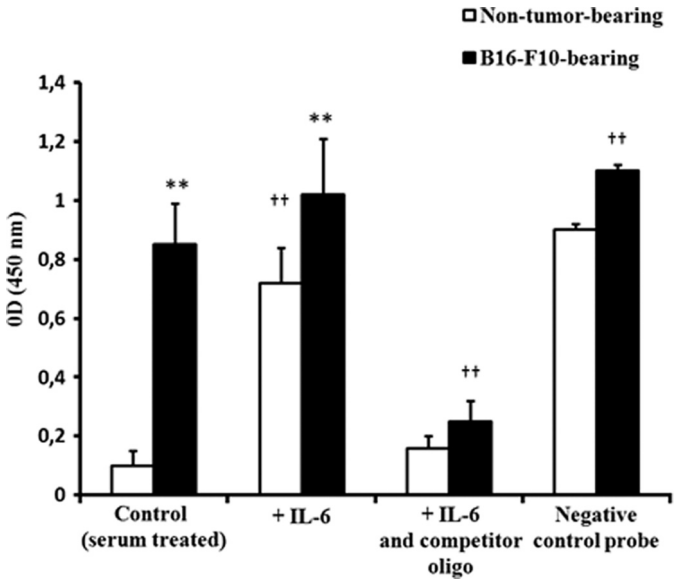

FIGURE 4. **STAT3 DNA binding activity in nuclear extracts of hepatocytes isolated from non-tumor-bearing or metastatic B16-F10 melanoma-bearing mice (lung metastases).** Nuclear extracts of hepatocytes isolated from B16-F10 (lung metastases)-bearing mice (10 days after tumor inoculation) or from non-tumor-bearing mice were prepared as described under "Experimental Procedures." Results are means ± S.D. (*error bars*) of 4–5 independent experiments. The significance test refers to the comparison between B16-F10- and non-tumor-bearing mice (**, $p < 0.01$), and all conditions *versus* controls (††, $p < 0.01$).

efflux significantly. In fact, as shown in Fig. 4, STAT3 DNA binding activity is ~8-fold higher in hepatocytes isolated from mice bearing B16-F10 metastases than in those isolated from non-tumor-bearing mice. However, IL-6 was only capable of increasing STAT3 DNA binding activity in hepatocytes isolated from non-tumor-bearing mice (Fig. 4) (and not in hepatocytes isolated from mice bearing B16-F10 metastases, where plasma levels of IL-6 are higher; see Fig. 1). Therefore, our results suggest that the hepatic GSH efflux mechanism in metastatic tumor-bearing mice is, at least in part, IL-6- and STAT3-dependent.

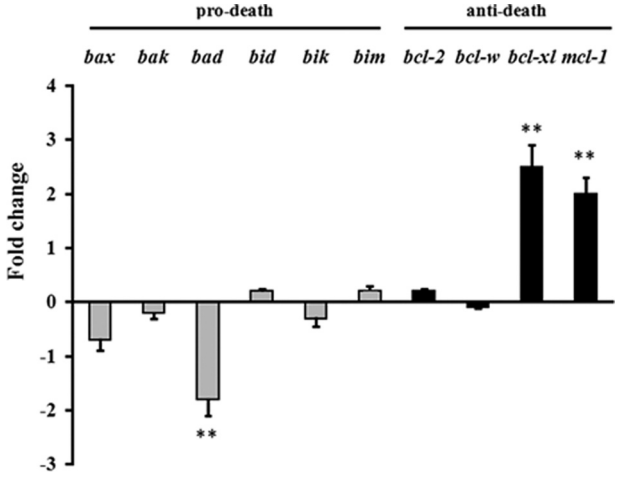

FIGURE 5. **Expression of pro-death and anti-death Bcl-2 genes in hepatocytes of metastatic B16-F10-bearing mice.** Hepatocytes were isolated from non-tumor- and tumor-bearing mice (lung metastases) by laser microdissection (as indicated under "Experimental Procedures") 10 days after tumor inoculation. The data, expressing -fold change (see "Experimental Procedures" for calculations), show mean values ± S.D. (*error bars*) for 5–6 different experiments (**, $p < 0.01$ for all genes displayed comparing hepatocytes from B16-F10-bearing mice (lung metastases) *versus* controls (hepatocytes from non-tumor-bearing mice, base line/-fold change = 0 in the figure).

Alteration of Death-related Mechanisms in Hepatocytes of B16-F10 Melanoma-bearing Mice—STAT3, besides modulating GSH efflux from hepatocytes in metastatic tumor-bearing mice (Fig. 3), is a vital protein that is activated by a number of ligands in addition to IL-6 (45). STAT3 has been shown to be involved in the transcriptional regulation of many genes (*e.g. IL-17*, *IL-23*, *bcl-xl*, *bcl-2*, *mcl1*, *ccnd1*, or *vegf*) (46), not only acting by direct DNA binding but acting in some cases as a coactivator of transcription factors, such as activator protein-1 and hepatocyte nuclear factor-1 (47). Furthermore, the anti-apoptotic proteins FLIP, Bcl-2, and Bcl-xL, which block caspase activation, have been found elevated in IL-6-treated livers (48). Moreover, these proteins were also found elevated in STAT3-overexpressing livers, thus providing evidence that STAT3 mediates the major antiapoptotic effects of IL-6. Therefore, because the Bcl-2 protein, in particular, has been postulated as a potential inhibitor of GSH efflux in HeLa (49) and B16-F10 cells (50), we finally measured expression of the Bcl-2 family of proteins in hepatocytes of non-tumor and B16-F10-bearing mice. As shown in Fig. 5, hepatocytes from B16-F10-bearing mice, as compared with hepatocytes from non-tumor-bearing mice, significantly down-regulate expression of *bad* and overexpress *bcl-xl* and *mcl-1*. In our experiments, Bcl-2 expression (Fig. 5) or levels (not shown) were not changed. These data indicate that gene transcription activation in hepatocytes of metastatic tumor-bearing mice, in addition to promoting GSH release to the blood, may also have other effects in the liver, such as protection against apoptosis. This protective effect, paradoxically, serves the tumor growth by ensuring hepatocyte survival and function.

DISCUSSION

Significant work has been done to delineate the intra- and extrahepatic (interorgan) turnover, transport, and disposal of GSH and to define the quantitative role of these processes in

interorgan homeostasis of GSH, Cys, and cystine. These studies have identified the liver as the central organ of interorgan GSH homeostasis, with sinusoidal GSH efflux as the major determinant of plasma GSH and thiol-disulfide status (3, 51–53).

GSH is synthesized from amino acid precursors (glutamate, cysteine, and glycine) in the cytosol of virtually all cells (13). This synthesis involves two ATP-requiring enzymatic steps. The first one, catalyzed by the γ-glutamylcysteine synthetase, is rate-limiting due to the very low concentration of cyst(e)ine in the cytosol (54). However, because there is no direct system for transport of intact GSH into cells, malignant cells might possibly utilize alternative pathways to ensure cyst(e)ine availability (55, 56). In addition, if extracellular levels of glutamate are high, as may occur in patients with advanced cancers, cystine uptake can be competitively inhibited, decreasing intracellular cyst(e)ine availability. Under these circumstances, cysteine released from extracellular GSH may play a crucial role in tumors expressing high GGT (34) able to degrade plasma GSH, thus providing an extra source of cysteine for uptake (13, 15). Therefore, systemic flow and delivery of GSH to these tumors (including not only melanoma but also, for example, human tumors of the liver, lung, breast, and ovary) (34) may favor their growth and resistance to chemoradiotherapy.

Malignant melanoma cells, as well as practically all cancer cells, can release different growth factors and cytokines, which (in addition of their autocrine and paracrine effects) are potential systemic signals (37). Because liver GSH appears depleted, as compared with non-tumor controls, in B16-F10-bearing mice (15), we investigated if the tumor itself releases molecular signals that may promote GSH release from the liver to the blood. Hepatic GSH depletion does not depend on the metastasis site; it occurs similarly in melanoma cells growing in the liver or in the lung (Table 2), and it is not the consequence of GSH synthesis inhibition but of an increased GSH efflux (Table 1). Fractionation of B16-F10 conditioned medium and neutralization assays identified IL-6 as a molecular factor capable of increasing GSH efflux from hepatocytes (Tables 3 and 4). IL-6 levels increase progressively in serum isolated from the blood of metastic B16-F10-bearing mice (Fig. 1), a fact that correlates with the increased rate of hepatic GSH efflux (Table 5), an increased rate that can be prevented by siRNA-induced tumor IL-6 silencing (Table 5) and that is channeled through a methionine-sensitive mechanism (Table 6). This methionine-sensitive transporter has been detected previously, but its molecular nature still remains to be defined (20, 57). Finally, IL-6-dependent signaling in hepatocytes (mainly JAK-STAT and MAPK pathways) was analyzed, and our results indicate that the increase in GSH efflux is STAT3-dependent (Figs. 2–4).

Inflammation is known to markedly impair hepatic detoxification pathways and thereby to alter pharmacokinetics of drugs (58). This has been linked to changes in liver expression of drug-metabolizing enzymes, such as cytochromes P450 (59) and more recently to that of drug transporters (60). In this sense, it has been suggested that proinflammatory cytokines, such as IL-1β, TNFα, and IL-6, may contribute to altered expression of hepatic drug transporters occurring during inflammation (61). Indeed, administration of IL-1β, TNFα, or IL-6 to rodents resulted in reduced expression of various sinusoidal or canalicular drug transporters (62–64). Moreover, as recently reported (65), exposure of primary human hepatocytes to 100 ng/ml TNFα or 10 ng/ml IL-6 for 48 h was found to down-regulate mRNA levels of major sinusoidal influx transporters, including sodium-taurocholate cotransporting polypeptide (NTCP), Oatp1, organic cation transporter 1 (OCT1), and organic anion transporter 2 (65). TNFα and IL-6 concomitantly reduced NTCP and Oatp1 protein expression and NTCP, Oatp1, and OCT1 transport activities. IL-6, but not TNFα, was also found to decrease mRNA expression of the canalicular transporters MDR1 and MRP2 (65). Nevertheless, we found previously that GSH efflux (2-fold higher than controls in hepatocytes from B16-F10-bearing mice) was not significantly inhibited by rifamycin SV or rifampicin (inhibitors of Oatp1 and/or Oatp2), although both inhibited taurocholate uptake (15). Besides, verapamil-induced inhibition or abrogation ($MRP1^{-/-}$, knock-out clone) of MRP1-dependent sinusoidal GSH efflux did not affect the rate of GSH release.[3] Moreover, sulfinpyrazone-induced inhibition or abrogation ($MRP2^{-/-}$, knock-out clone) of MRP2-dependent canalicular GSH efflux did not affect the rate of GSH release (15), thus suggesting the methionine-sensitive sinusoidal GSH efflux as the main mechanism for the effect observed in hepatocytes of melanoma-bearing mice. Nevertheless, apparently, different cytokines (see above) may alter several sinusoidal or canalicular drug transporters. This apparent paradox can be explained if one takes into account the difference between pathophysiological concentrations of those cytokines and the concentrations used in the reports mentioned above. As shown in Fig. 1, IL-6 levels in serum of B16-F10-bearing mice peak on day 10 after tumor inoculation up to ~700–900 pg/ml. We also measured TNFα levels and found a peak on day 10 after tumor inoculation of 151 ± 28 pg/ml ($n = 7$, $p < 0.01$) of serum in mice bearing B16-F10 lung metastases (*versus* a control value of 8 ± 3 pg/ml ($n = 7$) in non-tumor-bearing mice). Reports showing reduced expression of various sinusoidal and/or canalicular drug transporters (*e.g.* see Refs. 62 and 63 or Refs. 64 and 65) all used concentrations of cytokines in the nanomolar range, which are simply much higher than those found *in vivo*, at least in mice bearing B16-F10 metastases. To test this hypothesis, we measured taurocholate uptake in hepatocytes cultured (48 h) in the absence or in the presence of 900 pg of IL-6 and 150 pg of TNFα/ml (peak levels in serum of B16-F10-bearing mice; see above) and found similar rates: 231 ± 45 and 244 ± 37 nmol of taurocholate/g × min, respectively ($n = 5$). However, upon exposure of the same hepatocytes to 100 ng of TNFα/ml or 10 ng of IL-6/ml for 48 h (as described in Ref. 65), taurocholate uptake decreased to 77 ± 23 and 89 ± 33 nmol/g × min, respectively ($n = 5$, $p < 0.01$), thus showing that although, for example, Oatp1 activity can be influenced by two different cytokines in a concentration-dependent fashion, the concentration required appears much higher than that found in the blood stream of melanoma-bearing mice. Nevertheless, it is plausible that acute proinflammatory conditions, such as, for example, systemic viral or bacterial infections, may increase levels of circulating cytokines to the nanomolar range (*e.g.* see Ref. 66).

[3] J. M. Estrela, E. Obrador, and M. Benlloch, unpublished results.

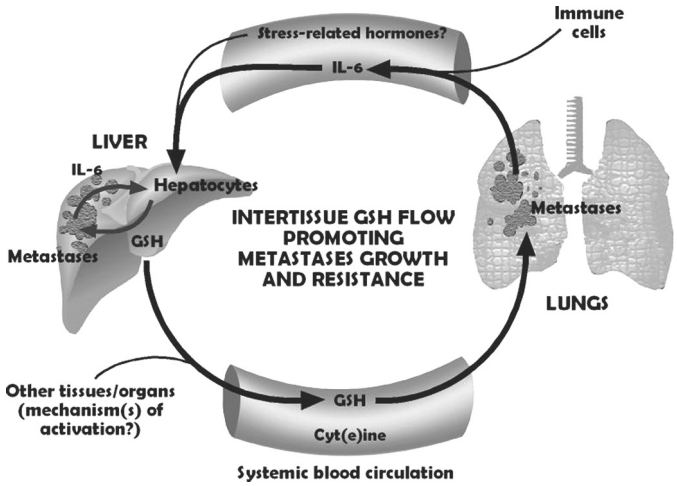

FIGURE 6. **The IL-6/GSH interorgan cycle: a tumor growth-promoting mechanism.** The liver is the major source of GSH released to the bloodstream. Tumor-derived IL-6 (and perhaps, under stress conditions, other signals, such as different stress-related hormones (1)) acts as a GSH release activator. Tumor GGT activity degrades plasma GSH, providing extra Cys for tumor GSH synthesis (12). Whether other tumor-derived signals activate hepatic GSH release in hosts bearing other cancer types and how each specific tissue microenvironment may influence this systemic flow are open questions.

In conclusion, Fig. 6 schematically summarizes the interorgan relationships linking tumor and liver functions and favoring metastases progression. Interestingly, cancer cell-associated IL-6 secretion has been linked to chemoresistance in different tumor types (67). Moreover, anticancer treatments, such as the chemotherapeutic agents doxorubicin or paclitaxel and radiation therapy, can also facilitate IL-6 release by tumor cells (68).

REFERENCES

1. Sies, H. (1999) *Free Radic. Biol. Med.* **27,** 916–921
2. Forman, H. J., Zhang, H., and Rinna, A. (2009) *Mol. Aspects Med.* **30,** 1–12
3. Estrela, J. M., Ortega, A., and Obrador, E. (2006) *Crit. Rev. Clin. Lab. Sci.* **43,** 143–181
4. Franco, R., Schoneveld, O. J., Pappa, A., and Panayiotidis, M. I. (2007) *Arch. Physiol. Biochem.* **113,** 234–258
5. Fidler, I. J. (1990) *Cancer Res.* **50,** 6130–6138
6. Weiss, L. (1990) *Adv. Cancer Res.* **54,** 159–211
7. Orr, F. W., Wang, H. H., Lafrenie, R. M., Scherbarth, S., and Nance, D. M. (2000) *J. Pathol.* **190,** 310–329
8. Li, L. M., Nicolson, G. L., and Fidler, I. J. (1991) *Cancer Res.* **51,** 245–254
9. Fidler, I. J. (1973) *Nat. New Biol.* **242,** 148–149
10. Carretero, J., Obrador, E., Esteve, J. M., Ortega, A., Pellicer, J. A., Sempere, F. V., and Estrela, J. M. (2001) *J. Biol. Chem.* **276,** 25775–25782
11. Anasagasti, M. J., Martin, J. J., Mendoza, L., Obrador, E., Estrela, J. M., McCuskey, R. S., and Vidal-Vanaclocha, F. (1998) *Hepatology* **27,** 1249–1256
12. Benlloch, M., Ortega, A., Ferrer, P., Segarra, R., Obrador, E., Asensi, M., Carretero, J., and Estrela, J. M. (2005) *J. Biol. Chem.* **280,** 6950–6959
13. Lu, S. C. (2009) *Mol. Aspects Med.* **30,** 42–59
14. Hanigan, M. H. (1995) *Carcinogenesis* **16,** 181–185
15. Obrador, E., Carretero, J., Ortega, A., Medina, I., Rodilla, V., Pellicer, J. A., and Estrela, J. M. (2002) *Hepatology* **35,** 74–81
16. Meister, A. (1983) *Science* **220,** 472–477
17. Zhang, H., Forman, H. J., and Choi, J. (2005) *Methods Enzymol.* **401,** 468–483
18. Meister, A. (1991) *Pharmacol. Ther.* **51,** 155–194
19. Ballatori, N., and Rebbeor, J. F. (1998) *Semin. Liver Dis.* **18,** 377–387
20. Ballatori, N., Krance, S. M., Marchan, R., and Hammond, C. L. (2009) *Mol. Aspects Med.* **30,** 13–28
21. Ballatori, N., Hammond, C. L., Cunningham, J. B., Krance, S. M., and Marchan, R. (2005) *Toxicol. Appl. Pharmacol.* **204,** 238–255
22. Carretero, J., Obrador, E., Anasagasti, M. J., Martin, J. J., Vidal-Vanaclocha, F., and Estrela, J. M. (1999) *Clin. Exp. Metastasis.* **17,** 567–574
23. Berry, M. N., and Friend, D. S. (1969) *J. Cell Biol.* **43,** 506–520
24. Singh, B., Borrebaek, B., and Osmundsen, H. (1983) *Acta. Physiol. Scand.* **117,** 497–505
25. Groen, A. K., Sips, H. J., Vervoorn, R. C., and Tager, J. M. (1982) *Eur. J. Biochem.* **122,** 87–93
26. New, L. S., and Chan, E. C. (2008) *J. Chromatogr. Sci.* **46,** 209–214
27. Asensi, M., Sastre, J., Pallardó, F. V., García de la Asunción, J., Estrela, J. M., and Viña, J. (1994) *Anal. Biochem.* **217,** 323–328
28. Bradford, M. M. (1976) *Anal. Biochem.* **72,** 248–254
29. Sale, E. M., Atkinson, P. G., and Sale, G. J. (1995) *EMBO J.* **14,** 674–684
30. Karras, J. G., McKay, R. A., Lu, T., Pych, J., Frank, D. A., Rothstein, T. L., and Monia, B. P. (2000) *Cell Immunol.* **202,** 124–135
31. Griffith, O. W., and Meister, A. (1979) *Proc. Natl. Acad. Sci. U.S.A.* **76,** 5606–5610
32. Terradez, P., Asensi, M., Lasso de la Vega, M. C., Puertes, I. R., Viña, J., and Estrela, J. M. (1993) *Biochem. J.* **292,** 477–483
33. Garibotto, G., Sofia, A., Saffioti, S., Russo, R., Deferrari, G., Rossi, D., Verzola, D., Gandolfo, M. T., and Sala, M. R. (2003) *Am. J. Physiol. Endocrinol. Metab.* **284,** E757–E763
34. Hochwald, S. N., Harrison, L. E., Rose, D. M., Anderson, M., and Burt, M. E. (1996) *J. Natl. Cancer Inst.* **88,** 193–197
35. Bannai, S., and Tateishi, N. (1986) *J. Membr. Biol.* **89,** 1–8
36. DeBerardinis, R. J., and Cheng, T. (2010) *Oncogene* **29,** 313–324
37. Lázár-Molnár, E., Hegyesi, H., Tóth, S., and Falus, A. (2000) *Cytokine* **12,** 547–554
38. Bhatia, S., Tykodi, S. S., and Thompson, J. A. (2009) *Oncology* **23,** 488–496
39. Stackpole, C. W., Groszek, L., and Kalbag, S. S. (1995) *Clin. Exp. Metastasis.* **13,** 105–115
40. Ilkovitch, D., and Lopez, D. M. (2008) *Exp. Dermatol.* **17,** 977–985
41. Gardell, S. J., and Tate, S. S. (1980) *FEBS. Lett.* **122,** 171–174
42. Deneke, S. M., and Fanburg, B. L. (1989) *Am. J. Physiol.* **257,** L163–L173
43. Heinrich, P. C., Behrmann, I., Haan, S., Hermanns, H. M., Müller-Newen, G., and Schaper, F. (2003) *Biochem. J.* **374,** 1–20
44. Singh, A., Jayaraman, A., and Hahn, J. (2006) *Biotechnol. Bioeng.* **95,** 850–862
45. Levy, D. E., and Lee, C. K. (2002) *J. Clin. Invest.* **109,** 1143–1148
46. Yu, H., Pardoll, D., and Jove, R. (2009) *Nat. Rev. Cancer.* **9,** 798–809
47. Leu, J. I., Crissey, M. A., Leu, J. P., Ciliberto, G., and Taub, R. (2001) *Mol. Cell Biol.* **21,** 414–424
48. Kovalovich, K., Li, W., DeAngelis, R., Greenbaum, L. E., Ciliberto, G., and Taub, R. (2001) *J. Biol. Chem.* **276,** 26605–26613
49. Meredith, M. J., Cusick, C. L., Soltaninassab, S., Sekhar, K. S., Lu, S., and Freeman, M. L. (1998) *Biochem. Biophys. Res. Commun.* **248,** 458–463
50. Ortega, A., Ferrer, P., Carretero, J., Obrador, E., Asensi, M., Pellicer, J. A., and Estrela, J. M. (2003) *J. Biol. Chem.* **278,** 39591–39599
51. Anderson, M. E., and Meister, A. (1980) *J. Biol. Chem.* **255,** 9530–9533
52. Ookhtens, M., Mittur, A. V., and Erhart, N. A. (1994) *Am. J. Physiol.* **266,** R979–R988
53. Ookhtens, M., and Kaplowitz, N. (1998) *Semin. Liver Dis.* **18,** 313–329
54. Griffith, O. W. (1999) *Free Radic. Biol. Med.* **27,** 922–935
55. O'Brien, M. L., and Tew, K. D. (1996) *Eur. J. Cancer.* **32A,** 967–978
56. van der Kolk, D. M., Vellenga, E., Müller, M., and de Vries, E. G. (1999) *Adv. Exp. Med. Biol.* **457,** 187–198
57. Fernández-Checa, J. C., García-Ruiz, C., Colell, A., Yi, J. R., and Kaplowitz, N. (1996) *Am. J. Physiol.* **270,** G969–G975
58. Slaviero, K. A., Clarke, S. J., and Rivory, L. P. (2003) *Lancet Oncol.* **4,** 224–232
59. Renton, K. W. (2004) *Curr. Drug. Metab.* **5,** 235–243
60. Morgan, E. T., Goralski, K. B., Piquette-Miller, M., Renton, K. W., Robertson, G. R., Chaluvadi, M. R., Charles, K. A., Clarke, S. J., Kacevska, M., Liddle, C., Richardson, T. A., Sharma, R., and Sinal, C. J. (2008) *Drug. Metab. Dispos.* **36,** 205–216

61. Hartmann, G., Cheung, A. K., and Piquette-Miller, M. (2002) *J. Pharmacol. Exp. Ther.* **303,** 273–281
62. Green, R. M., Beier, D., and Gollan, J. L. (1996) *Gastroenterology* **111,** 193–198
63. Siewert, E., Dietrich, C. G., Lammert, F., Heinrich, P. C., Matern, S., Gartung, C., and Geier, A. (2004) *Biochem. Biophys. Res. Commun.* **322,** 232–238
64. Geier, A., Dietrich, C. G., Voigt, S., Ananthanarayanan, M., Lammert, F., Schmitz, A., Trauner, M., Wasmuth, H. E., Boraschi, D., Balasubramaniyan, N., Suchy, F. J., Matern, S., and Gartung, C. (2005) *Am. J. Physiol. Gastrointest. Liver Physiol.* **289,** G831–G841
65. Vee, M. L., Lecureur, V., Stieger, B., and Fardel, O. (2009) *Drug. Metab. Dispos.* **37,** 685–693
66. Damas, P., Ledoux, D., Nys, M., Vrindts, Y., De Groote, D., Franchimont, P., and Lamy, M. (1992) *Ann. Surg.* **215,** 356–362
67. Wang, Y., Niu, X. L., Qu, Y., Wu, J., Zhu, Y. Q., Sun, W. J., and Li, L. Z. (2010) *Cancer Lett.* **295,** 110–123
68. Emmenegger, U., and Kerbel, R. S. (2010) *Nature* **468,** 637–638